Research on the Estimation of the Flexural Capacity of EPS Lightweight Concrete Panels

Sy-Dan Dao
University of Transport and Communications, Vietnam
sydandao@utc.edu.vn (corresponding author)

Received: 25 September 2024 | Revised: 20 October 2024 | Accepted: 3 November 2024

 DOI: https://doi.org/10.48084/etasr.9091

ABSTRACT

Expanded Polystyrene (EPS) lightweight concrete possesses numerous special characteristics, including exceptionally low weight, good sound insulation, effective heat insulation, great fire resistance, and low water absorption. Consequently, it has garnered significant attention for research and practical applications in the construction industry, particularly in the development of soundproofing and thermal insulation components, as well as lightweight elements to reduce the superstructure weight, such as external wall panels, floor slabs, roof panels, and base materials. The primary objective of this study is to analyze and estimate the flexural capacity of EPS lightweight concrete panels through both experimental and numerical methods. Furthermore, the influence of the longitudinal reinforcement ratio, strength, and thickness of EPS lightweight aggregate concrete panels on their flexural capacity is thoroughly investigated and evaluated. The findings demonstrate that the Abaqus software, with an appropriate material model for EPS lightweight aggregate concrete, can reliably predict the flexural capacity of EPS lightweight concrete panels reinforced with longitudinal rebars.

Keywords-EPS lightweight concrete; flexural capacity; experimental test; numerical model

I. INTRODUCTION

EPS lightweight aggregate concrete was extensively researched and applied worldwide during the 1970s. This material possesses several advantages, including low dry density, ranging from 500 kg/m^3 to 1800 kg/m^3 depending on the amount of EPS particles used, sound and thermal insulation, fire resistance, and low water absorption. Consequently, the usage of such concrete in construction projects can significantly reduce the load on building foundations and result in substantial energy savings, while its production contributes to mitigating environmental pollution. EPS lightweight aggregate concrete has gathered substantial attention for research and practical applications in the construction industry since its discovery, with various issues related to its physical and mechanical properties, as well as its applicability in construction having been explored. These studies have investigated factors like dry density, compressive strength, tensile strength, sound insulation, thermal insulation, water absorption, and construction techniques.

Several studies have investigated EPS lightweight concrete with compressive strengths ranging from 7.5 MPa to 62.6 MPa, and have explored the effect of EPS particle size and gradation on the compressive and flexural strengths [1]. Previous research has examined the impact of EPS content on the fire resistance, thermal conductivity, and compressive strength of foam concrete [2]. Foam concrete was supplemented with lightweight EPS aggregate particles to achieve a dry density between 150 kg/m³ and 400 kg/m³. The results indicated that the thermal conductivity, fire resistance, compressive strength, and density of foam concrete decrease significantly when EPS particles are incorporated. The application of EPS lightweight concrete for the outer layer of barrier members used as rigid separators on highways, demonstrated that these barrier members effectively absorbed impact forces from vehicles [3]. The flexural and compressive capacities of unreinforced EPS lightweight concrete panels with dry densities ranging from 650 kg/m³ to 750 kg/m³ have been also evaluated [4].

Additionally, the effects of using EPS particles as coarse aggregate on the fire resistance, water absorption, and compressive strength of EPS lightweight concrete, as well as the materials' potential as load-bearing panel components and base materials in construction has been examined [5]. Using 75 mm thick EPS lightweight concrete panels as thermal insulation roof panels can reduce material costs, carbon emissions, and energy consumption by 8.3%, 20%, and 41%, respectively, in addition to their environmental benefits [6]. The influence of the amount of EPS particles added to aerated concrete on the mechanical properties, including compressive strength, flexural strength, and modulus of elasticity, has also been investigated [7]. Further research has examined the effect of the volume ratio of EPS particles replacing coarse aggregate on the physical and mechanical properties of EPS lightweight concrete, such as density, flexural strength, and compressive strength [8]. Lastly, the flexural behavior of lightweight self-compacted concrete beams made from EPS lightweight concrete and reinforced with rebars and steel fibers has been experimentally investigated, with a focus on the volume ratio of EPS particles and steel fibers replacing coarse aggregate [9].

Existing research has primarily focused on the manufacturing technology, the physical, and mechanical attributes of EPS lightweight concrete. While a small number of research endeavors have examined the flexural behavior of lightweight concrete panels, they have been confined to EPS lightweight concrete panels without reinforcement. This paper aims to evaluate the flexural capacity of EPS lightweight concrete panels through both experimental and numerical analyses. Furthermore, the study explores the influence of key factors, such as the longitudinal reinforcement ratio, the strength of EPS lightweight concrete, and the thickness of the panels, on their flexural performance.

II. EXPERIMENTAL TEST

This section presents an experimental test to determine the flexural capacity of EPS lightweight concrete panels reinforced with longitudinal reinforcement. Three identical EPS lightweight concrete panels with primary longitudinal reinforcement were subjected to four-point bending tests to evaluate their flexural capacity. These EPS lightweight concrete panels had dimensions of 2000 mm in length, 500 mm in width, and 100 mm in thickness; they were produced from EPS lightweight concrete with a density of 900 kg/m³ and a compressive strength of 3.2 MPa, respectively. The longitudinal reinforcement in both the top and bottom layers comprised three bars, each with a diameter of 3 mm and a yield strength of 485 MPa. The four-point bending test setup is illustrated in Figure 1.

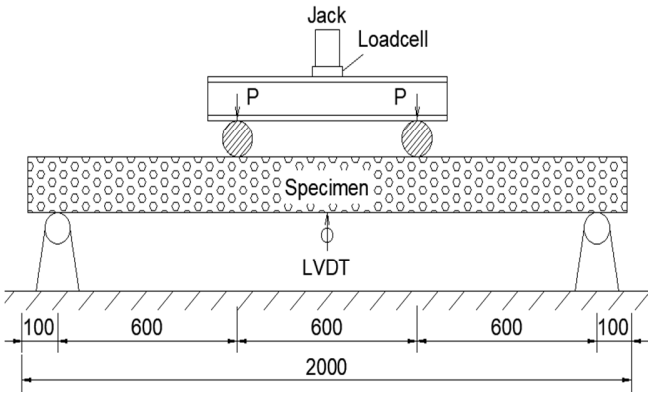

Fig. 1. Schematic of the four-point bending test setup.

The loading is applied in a stepwise manner until the sample fails. Each load increment is set at approximately one-tenth of the load that causes sample failure. The load is maintained for a minimum of 5 minutes for low load levels and a minimum of 10 minutes for high load levels. For the final load increments, the loading should be only increased once the measurements from the displacement and force gauges have been stabilized. During the testing process, it is crucial to closely observe the specimen's behavior, including the formation and propagation of transverse cracks in the regions experiencing significant bending moments, as well as the deflection of the specimen at the mid-span cross-section. Figure 2 below depicts an actual image of the sample that has deflected and developed numerous transverse cracks in the region experiencing significant bending. These transverse cracks appear at relatively uniform intervals, which is consistent with the behavior observed in normal reinforced concrete slabs under bending.

Fig. 2. Actual image of the sample showing deflection and cracking under bending.

III. NUMERICAL MODEL AND VALIDATION

In this section, the four-point bending test to failure for the EPS lightweight concrete panel will be simulated numerically using Abaqus CAE 2019. Abaqus is one of the most widely used finite element analysis software programs today, developed since 1978 by Dassault Systèmes Simulia, in the USA. It is a powerful computational tool used to numerically simulate many practical engineering problems based on the finite element method, such as structural analysis problems, heat transfer problems, electromagnetic problems, acoustic problems, piezoelectric problems, geotechnical problems, and fluid dynamics problems. It can address problems ranging from simple linear analysis to the most complex nonlinear simulations.

A. Numerical Model

Given the relatively simple nature and small scale of the experimental sample, the entire model can be fully simulated using Abaqus software. The EPS lightweight concrete panel is represented as a solid three-dimensional block with C3D8R elements. The primary longitudinal reinforcement is modeled as one-dimensional bars in three-dimensional space with T3D2 elements. The transverse reinforcement bars have a negligible impact on the flexural capacity of the panel, and their modeling is avoided. As the deformations of the supports and load transfer beams are minor compared to the deformations of the EPS panel, they are modeled as completely rigid elements.

Abaqus provides three types of constitutive models to simulate the concrete behavior, including elastic behavior, plastic behavior, and failure mechanisms. These are the brittle crack model, smeared crack model, and Concrete Damaged Plasticity model (CDP). The brittle crack model only considers the nonlinear behavior of concrete under tension. This model assumes that concrete behaves as linear elastic under compression, making it suitable for simulating unreinforced concrete structures or lightly reinforced concrete structures. However, it is not suitable for normal reinforced concrete

structures [10]. The smeared crack model is applied to homogenize the discrete cracks of concrete in reality. The CDP model can be used to simulate the fundamental behavior of concrete under cyclic loading and the degradation of concrete stiffness under the influence of cyclic loading. This model accounts for two failure mechanisms of concrete: cracking under tensile stress and crushing under compressive stress. A continuous failure mechanism is employed to simulate crack propagation and crack growth through a stiffness degradation approach, where the stiffness of the concrete gradually decreases as it cracks. In this study, the CDP model is used to simulate lightweight EPS concrete. The input parameters for the CDP model include:

- The stress-strain curve of concrete under uniaxial compression and uniaxial tension.
- Damage parameters under uniaxial compression and tension.
- Plasticity flow parameters, including: dilation angle (ψ), eccentricity (ϵ), stress ratio (σ_{bo}/σ_{co}), shape factor (K_c), and viscosity parameter (μ).

The stress-strain curves for concrete under uniaxial compression and tension can be assumed, as illustrated in Figures 3 and 4 [11].

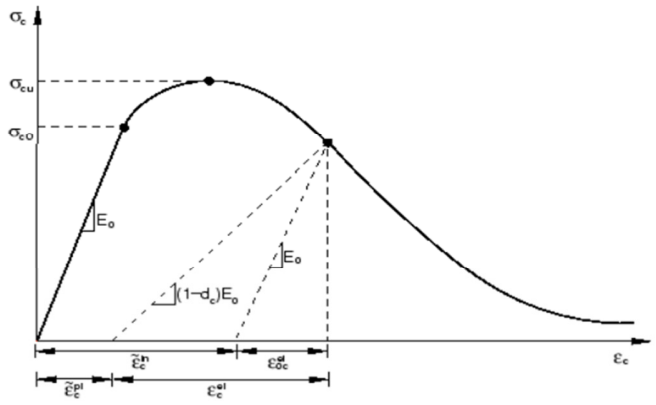

Fig. 3. Stress-strain curve and related parameters for normal concrete under uniaxial compression.

In Figure 3, under uniaxial compression, the stress-strain response of concrete exhibits linear elastic behavior up to the elastic compressive strength (σ_{co}). The elastic compressive strength can be determined using (1) where σ_{cu} is the ultimate compressive strength of the concrete [12]. Additionally, the modulus of elasticity of concrete can be calculated using (2). Beyond the elastic limit, the concrete undergoes plastic deformation, characterized by a stress hardening curve, followed by a softening curve once the ultimate compressive stress (σ_{cu}) is surpassed. The stress-strain relationship in the plastic region is parabolic and can be expressed using (3) [12]. For normal concrete, ultimate stress (ϵ_o) can be taken as 0.002 and ultimate strain (ϵ_u) as 0.003 [13].

$$\sigma_{co} = 0.6\sigma_{cu} \quad (1)$$

$$E_o = 4700\sqrt{f_c'}(MPa) \quad (2)$$

$$\sigma_c = \sigma_{cu}[\frac{2\varepsilon_o}{\varepsilon_o} - (\frac{\varepsilon_o}{\varepsilon_o})^2] \quad (3)$$

The dry density γ_c of EPS lightweight concrete ranges from 800 kg/m^3 to 1200 kg/m^3 [14]. The stress-strain curve under uniaxial compression is represented by (4) for the stress hardening branch and (5) for the stress softening branch. The values of the parameters in these equations depend on the dry density of the concrete and are determined using (6) through (9), accordingly. The strain corresponding to ϵ_o was found to be between 0.0035 and 0.0051, while ϵ_u was approximately 0.012.

$$\sigma_c = \sigma_{cu}\left[\frac{a(\frac{\varepsilon_c}{\varepsilon_o})+(b-1)(\frac{\varepsilon_c}{\varepsilon_o})^2}{1+(a-2)(\frac{\varepsilon_c}{\varepsilon_o})+(b-1)(\frac{\varepsilon_c}{\varepsilon_o})^2}\right] \quad (4)$$

$$\sigma_c = \sigma_{cu}\left[\frac{1+c}{(\frac{\varepsilon_c}{\varepsilon_o})^d+c}\right] \quad (5)$$

$$a = 0.961\gamma_c^2 10^{-6} - 0.0026\gamma_c + 2.189 \quad (6)$$

$$b = 1.218\gamma_c^2 10^{-6} - 0.0016\gamma_c + 0.967 \quad (7)$$

$$c = -7.275\gamma_c^2 10^{-6} + 0.0161\gamma_c - 10.503 \quad (8)$$

$$d = -11.301\gamma_c^2 10^{-6} + 0.0135\gamma_c - 5.080 \quad (9)$$

Using the above equations, the stress-strain relation for EPS lightweight concrete under uniaxial compression can be determined, as illustrated in Figure 4.

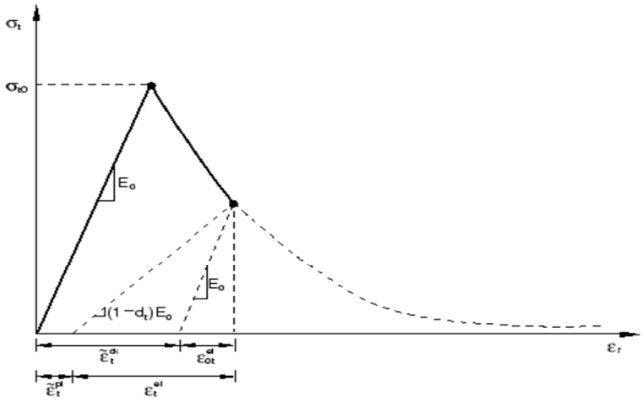

Fig. 4. Stress-strain curve and related parameters for normal concrete under uniaxial tension.

Figure 5 illustrates that concrete under uniaxial tension initially exhibits linear elastic behavior up to its ultimate tensile strength (σ_{to}) followed by a plastic deformation region characterized by stress softening. The ultimate tensile strength of EPS lightweight concrete can be determined using (10) [15]. Furthermore, the stress-strain curve beyond the ultimate tensile strength for normal concrete can be calculated by (11) [16].

$$\sigma_{to} = 0.301\sigma_{cu}^{0.684} \quad (10)$$

$$\sigma_t = \frac{\sigma_{to}}{1+\sqrt{500\varepsilon_t}} \quad (11)$$

Thus, the stress-strain relation for EPS lightweight concrete under uniaxial tension can be determined, as shown in Figure 6.

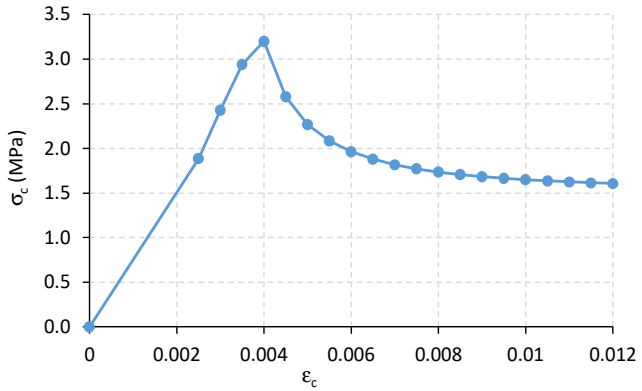

Fig. 5. Stress-strain relation for EPS lightweight concrete under uniaxial compression.

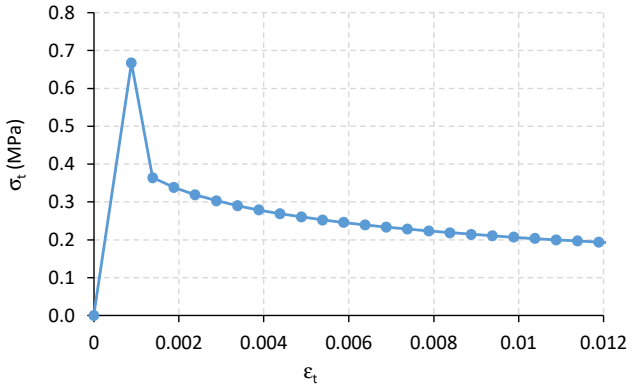

Fig. 6. Stress-strain relation for EPS lightweight concrete under uniaxial tension for present study.

From Figure 3, the inelastic compressive strain (ϵ_c^{in}) and the cracking strain (ϵ_t^{ck}), using (12) and (13) respectively, can be easily determined. Here, ϵ_{oc}^{el} and ϵ_{ot}^{el} are the corresponding elastic compressive and tensile strains, which can be calculated using (14) and (15), respectively.

$$\varepsilon_c^{in} = \varepsilon_c - \varepsilon_{oc}^{el} \quad (12)$$

$$\varepsilon_t^{ck} = \varepsilon_t - \varepsilon_{ot}^{el} \quad (13)$$

$$\varepsilon_{oc}^{el} = \frac{\sigma_c}{E_o} \quad (14)$$

$$\varepsilon_{ot}^{el} = \frac{\sigma_t}{E_o} \quad (15)$$

Under cyclic loading, the modulus of elasticity or stiffness of concrete in the plastic deformation region typically decreases compared to the initial modulus of elasticity (E_o). The reduction in the modulus of elasticity of concrete under cyclic loading is characterized by the compressive damage parameter (d_c) and the tensile damage parameter (d_t). In Figure 3, the elastic modulus of concrete in the plastic deformation region under cyclic loading can be calculated from (16) and (17), respectively. The compressive and tensile damage parameters are customarily determined through experimentation. In the absence of experimental data, these damage parameters can be estimated using (18) and (19) [17-19].

$$E_c = (1 - d_c)E_o \quad (16)$$

$$E_t = (1 - d_t)E_o \quad (17)$$

$$d_c = 1 - \frac{\sigma_c}{\sigma_{cu}} \quad (18)$$

$$d_t = 1 - \frac{\sigma_t}{\sigma_{to}} \quad (19)$$

From the d_c and d_t, the plastic strains due to compression and tension can be easily determined using (20) and (21), respectively.

$$\varepsilon_c^{pl} = \varepsilon_c^{in} - \frac{d_c}{1-d_c} \cdot \frac{\sigma_c}{E_o} \quad (20)$$

$$\varepsilon_t^{pl} = \varepsilon_t^{ck} - \frac{d_t}{1-d_t} \cdot \frac{\sigma_t}{E_o} \quad (21)$$

The fourth parameter is the shape factor (K_c), which is the ratio of the second stress invariant on the tensile meridian to that on the compressive meridian at the initial yield point. The value of K_c must satisfy the condition $0.5 < K_c \leq 1.0$, and it is taken as a default value of 0.667. The final parameter is the viscosity parameter (μ), which allows the stress to slightly exceed the yield surface so that the computational process converges more quickly. The smaller the value of the viscosity parameter is, the more accurate the results will be, and vice versa. According to [18], the viscosity parameter can range from 0.0001 to 0.008; in this study, it is taken as 0.001.

The plastic flow parameters can be specified as: ψ, which is used to define the behavior of concrete under confined stress, and is recommended to be within the range of 30 to 45 degrees, with a suggested value of 40 degrees for lightweight EPS concrete [18]. The parameter ϵ, which describes the ratio between tensile and compressive strength, is recommended to be 0.1. The third parameter σ_{bo}/σ_{co} 1 is recommended to be between 1.00 and 1.16, with a suggested value of 1.16 for this study. The fourth parameter K_c must satisfy the condition $0.5 < K_c < 1.0$, and is taken as a default of 0.667. The final parameter μ, can range from 0.0001 to 0.008, with a value of 0.001 used for this study [18]. The input parameters for EPS lightweight concrete are displayed in Table I.

TABLE I. ELASTIC AND PLASTIC FLOW PARAMETERS FOR LIGHTWEIGHT EPS CONCRETE

No.	Parameters	Values	Units
1	E_o	800	MPa
2	ν	0.3	-
3	ψ	40	Degree
4	ϵ	0.1	-
5	σ_{bo}/σ_{co}	1.16	-
6	K_c	0.667	-
7	μ	0.001	-

The reinforcing steel used for the EPS panel in this study has a yield strength of 485 MPa. According to [13], it can be assumed that the steel is an elastic – perfectly plastic model, as depicted in Figure 7. Based on this, the input parameters for the reinforcing steel are obtained, as presented in Table II.

The reinforcing steel employed in the EPS panel for this study highlights a yield strength of 485 MPa. As depicted in Figure 7, it is assumed that the steel demonstrates an elastic-

perfectly plastic behavior [13]. Accordingly, the input parameters for the reinforcing steel utilized are presented in Table II below.

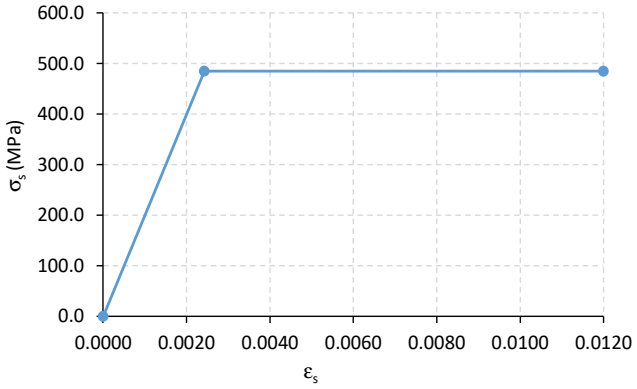

Fig. 7. Stress-strain relation for uniaxial tension of the idealized rebars in Abaqus.

TABLE II. INPUT PARAMETERS FOR THE REINFORCING STEEL

No.	Parameters	Values	Units
1	E_s	2.10^5	MPa
2	ν	0.3	-
3	f_y	485	MPa

Bonding between rebars and concrete is critically important, as it ensures the collaborative interaction between the two materials. Without sufficient bond force, the rebars would slip out of the concrete under load. Given that the rebars used are ribbed steel, the bond strength between the rebars and concrete is presumed to be adequately large to prevent sliding when subjected to force. Accordingly, the embedded element technique can be employed to simulate the bond between the rebars and concrete. When this technique is utilized, the translational degrees of freedom of the nodes in the embedded element are constrained to the interpolated values of the corresponding degrees of freedom in the host element.

The lightweight EPS concrete panel undergoes four-point bending until complete failure, enabling the assessment of its flexural capacity. The panel rests on supports at both ends, with one end acting as a pinned support and the other as a roller support. The pushover technique is employed to determine the panel's flexural capacity, subjecting it to forced displacement at the loading points until failure. Furthermore, the reference point and rigid body techniques are utilized to constrain the displacement of the reference points with the supports. In this case, the boundary conditions of the supports only require definition for the reference points. This approach facilitates the efficient determination of the support reactions, which are equivalent to the loads applied to the panel.

B. Validation

The numerical analysis conducted using Abaqus software produced results, as illustrated in Figures 8 and 9, that exhibited a symmetrical concave pattern in the vertical displacement (*U2*) of the sample. Furthermore, the tensile failure zone was observed to be symmetrically distributed within the region characterized by significant bending moments, aligning with the experimental observations.

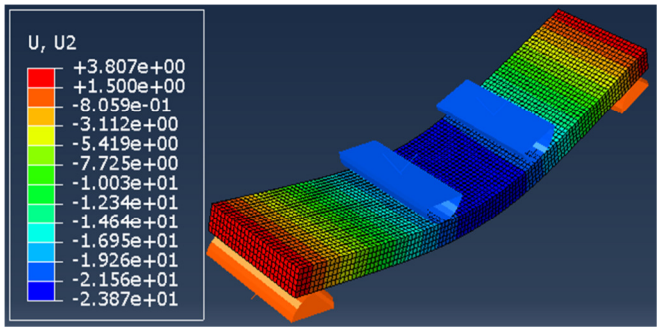

Fig. 8. Image of the vertical displacement distribution *U2* in mm of the EPS panel.

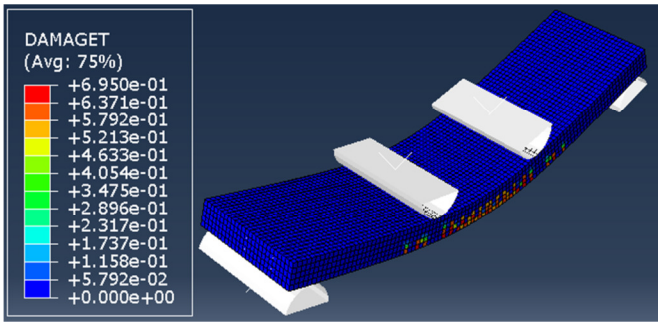

Fig. 9. Image of the tension damage region of the EPS panel.

Figure 10 portrays the comparison of the relationship curve between the bending load (*P*) and the *U2* at the mid-span cross-section obtained from the experiment and numerical analysis during the bending failure test of the sample. The results indicate that the relationship curves from the two approaches are highly similar. Specifically, the discrepancy between the maximum bending load and the vertical displacement at the mid-span cross-section is small. The P-U2 relationship curve exhibits two distinct stages; the first one is the linear elastic stage when the bending load is still small and the second one refers to the inelastic linear stage with reduced stiffness, commencing when the tensile concrete zone begins to crack until the tensile reinforcement starts yielding.

However, at stage 3, characterized by rapid plastic deformation until failure, this is not clearly observed. This may be attributed to the longitudinal reinforcement ratio being too low or the panel thickness being insufficient compared to typical reinforced concrete beams. Additionally, the *P-U2* relationship curve from the experiments displays local descending segments, a consequence of the incremental loading approach employed, where each load increment was maintained for approximately 5 to 10 minutes. In conclusion, the proposed numerical model can be considered reliable for conducting further studies.

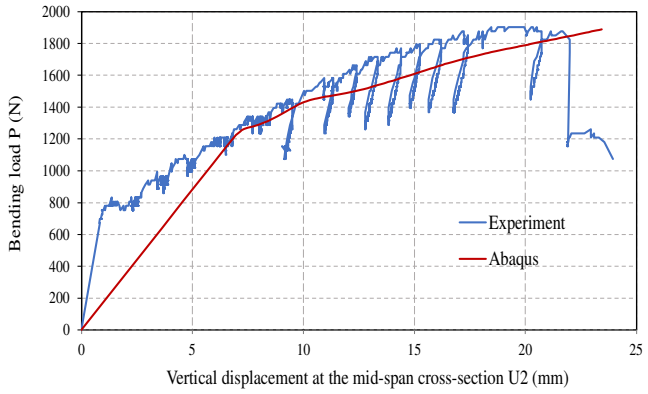

Fig. 10. *P-U2* relationship curve.

IV. PERAMETRIC STUDIES AND RESULTS

This section examines and assesses the flexural performance of the lightweight EPS concrete panel, and its impact of varying factors, such as the quantity of longitudinal reinforcement, concrete compressive strength, and panel thickness.

A. Effect of Longitudinal Reinforcement Content

The longitudinal reinforcement ratio was adjusted by changing the number and diameter of the longitudinal reinforcement rebars. The analysis focused on the typical design range for reinforced concrete slabs, which is between a 0.05% and 2% longitudinal reinforcement ratio.

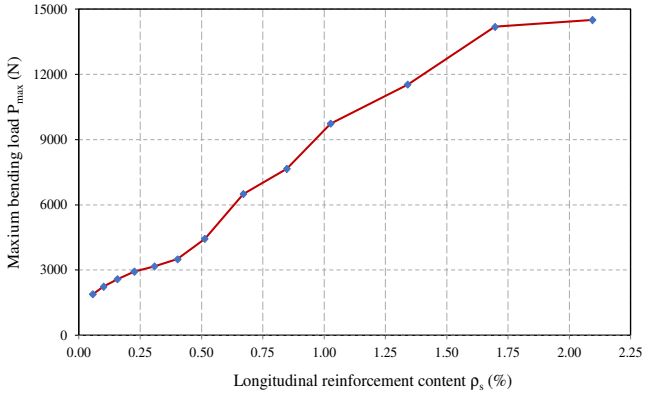

Fig. 11. Effect of longitudinal reinforcement content on the flexural capacity of the EPS panel.

The results, as depicted in Figure 11, demonstrate that as the longitudinal reinforcement ratio increases from 0.06% to 1.7%, the maximum bending load of the panel rises almost linearly from 1889 N to 14494 N. Beyond the 1.7% longitudinal reinforcement ratio, the maximum bending load continues to increase linearly, but with a smaller slope.

B. Effect of Lightweight EPS Concrete Strength

Typically, the compressive strength of EPS lightweight concrete ranges from 1.6 MPa to 8 MPa. As illustrated in Figure 12, as the compressive strength of the EPS lightweight concrete increases from 1.6 MPa to 8 MPa, the maximum bending load of the panel exhibits an almost linear increase from 1150 N to 3819 N.

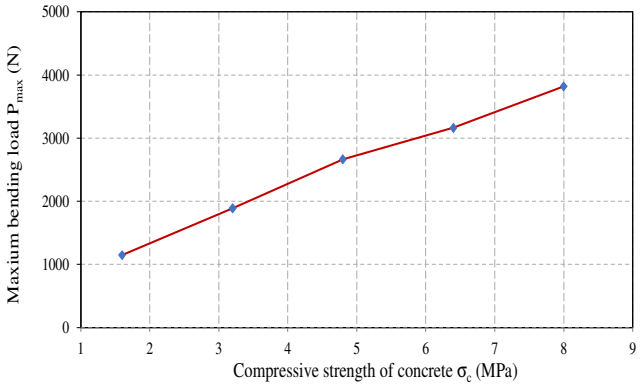

Fig. 12. Effect of concrete strength on the flexural capacity of the EPS panel.

C. Effect of the Thickness of the Lightweight EPS Concrete Panel

The position of the longitudinal reinforcement bars must be maintained at a fixed distance of 25 mm from both the top and bottom surfaces of the panel, regardless of the thickness changes. To ensure sufficient longitudinal reinforcement, the study will examine a case where both the upper and lower longitudinal reinforcement consist of 5 D5 bars each.

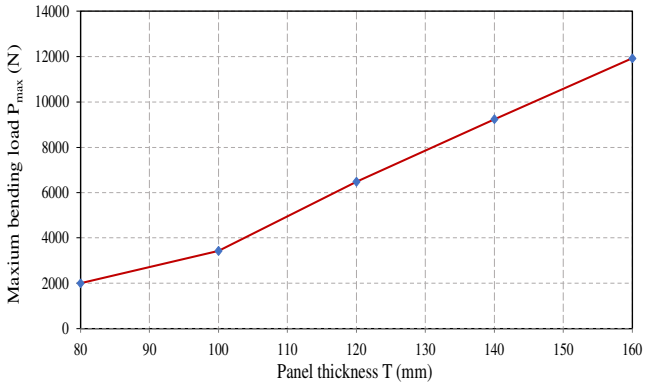

Fig. 13. Effect of panel thickness on the flexural capacity of the EPS Panel.

Since typical floor slabs range in thickness from 80 mm to 160 mm, the EPS lightweight concrete panel will be studied within this thickness range. Figure 13 displays that as the panel thickness increases from 80 mm to 160 mm, the maximum bending load of the panel increases almost linearly from 2003 N to 11927 N.

V. CONCLUSIONS

Expanded Polystyrene (EPS) lightweight aggregate concrete has may outstanding advantages. However, previous studies solely focused on the technology for producing EPS lightweight concrete and its physical and mechanical properties. This article estimates the flexural capacity of EPS lightweight concrete panels reinforced with longitudinal steel

bars through both experimental and numerical analysis. Several conclusions were drawn:

- The Abaqus software, with an appropriate material model, can reasonably predict the flexural capacity of the EPS lightweight concrete panel reinforced with longitudinal reinforcement.
- When the longitudinal reinforcement ratio increases from 0.06% to 1.7%, the maximum bending load of the panel increases almost linearly from 1889 N to 14494 N. When the longitudinal reinforcement ratio exceeds 1.7%, the maximum bending load of the panel continues to increase linearly but with a smaller slope.
- When the compressive strength of EPS lightweight concrete increases from 1.6 MPa to 8 MPa, the maximum bending load of the panel increases almost linearly from 1150 N to 3819 N.
- When the thickness of lightweight concrete panel increases from 80 mm to 160 mm, the maximum bending load of the panel increases almost linearly from 2003 N to 11927 N.

ACKNOWLEDGMENT

This research is funded by University of Transport and Communications (UTC), Vietnam.

REFERENCES

[1] N. Liu and B. Chen, "Experimental study of the influence of EPS particle size on the mechanical properties of EPS lightweight concrete," *Construction and Building Materials*, vol. 68, pp. 227–232, Oct. 2014, https://doi.org/10.1016/j.conbuildmat.2014.06.062.

[2] A. A. Sayadi, J. V. Tapia, T. R. Neitzert, and G. C. Clifton, "Effects of expanded polystyrene (EPS) particles on fire resistance, thermal conductivity and compressive strength of foamed concrete," *Construction and Building Materials*, vol. 112, pp. 716–724, Jun. 2016, https://doi.org/10.1016/j.conbuildmat.2016.02.218.

[3] H. J. Mohammed and M. F. M. Zain, "Experimental application of EPS concrete in the new prototype design of the concrete barrier," *Construction and Building Materials*, vol. 124, pp. 312–342, Oct. 2016, https://doi.org/10.1016/j.conbuildmat.2016.07.105.

[4] P. L. N. Fernando, M. T. R. Jayasinghe, and C. Jayasinghe, "Structural feasibility of Expanded Polystyrene (EPS) based lightweight concrete sandwich wall panels," *Construction and Building Materials*, vol. 139, pp. 45–51, May 2017, https://doi.org/10.1016/j.conbuildmat.2017.02.027.

[5] N. H. Ramli Sulong, S. A. S. Mustapa, and M. K. Abdul Rashid, "Application of expanded polystyrene (EPS) in buildings and constructions: A review," *Journal of Applied Polymer Science*, vol. 136, no. 20, Jan. 2019, Art. no. 47529, https://doi.org/10.1002/app.47529.

[6] D. P. P. Meddage, A. Chadee, M. T. R. Jayasinghe, and U. Rathnayake, "Exploring the applicability of expanded polystyrene (EPS) based concrete panels as roof slab insulation in the tropics," *Case Studies in Construction Materials*, vol. 17, Dec. 2022, Art. no. e01361, https://doi.org/10.1016/j.cscm.2022.e01361.

[7] R. Shabbar, A. A. Al-Tameemi, and A. M. J. Alhassani, "The effect of expanded polystyrene beads (EPS) on the physical and mechanical properties of aerated concrete," *Open Engineering*, vol. 12, no. 1, pp. 424–430, Jun. 2022, https://doi.org/10.1515/eng-2022-0020.

[8] A. S. Salahaldeen and A. I. Al-Hadithi, "The Effect of Adding Expanded Polystyrene Beads (EPS) on the Hardened Properties of Concrete," *Engineering, Technology & Applied Science Research*, vol. 12, no. 6, pp. 9692–9696, Dec. 2022, https://doi.org/10.48084/etasr.5278.

[9] R. M. Abbas and R. K. Rakaa, "Structural Performance of Lightweight Fiber Reinforced Polystyrene Aggregate Self-Compacted Concrete Beams," *Engineering, Technology & Applied Science Research*, vol. 13, no. 5, pp. 11865–11870, Oct. 2023, https://doi.org/10.48084/etasr.6217.

[10] Y.-H. Wang, Q. Tang, and X. Nie, "Comparative investigation on influences of concrete material constitutive models on structural behavior," *Construction and Building Materials*, vol. 144, pp. 475–483, Jul. 2017, https://doi.org/10.1016/j.conbuildmat.2017.03.174.

[11] *Abaqus 6.14 – Analysis user's guide*, vol. 5. Providence, RI, USA: Dassault Systèmes, 2014.

[12] M. P. Collins and D. Mitchell, *Prestressed Concrete Structure*, 2nd ed. Toronto, Canada: Response Publications, 1997.

[13] *318-19(22): Building Code Requirements for Structural Concrete and Commentary,* ACI Committee 318, MI, USA, 2019.

[14] C. Cui, Q. Huang, D. Li, C. Quan, and H. Li, "Stress–strain relationship in axial compression for EPS concrete," *Construction and Building Materials*, vol. 105, pp. 377–383, Feb. 2016, https://doi.org/10.1016/j.conbuildmat.2015.12.159.

[15] Y. Xu, L. Jiang, J. Xu, H. Chu, and Y. Li, "Prediction of compressive strength and elastic modulus of expanded polystyrene lightweight concrete," *Magazine of Concrete Research*, vol. 67, no. 17, pp. 954–962, Sep. 2015, https://doi.org/10.1680/macr.14.00375.

[16] R. M. Barker and J. A. Puckett, *Design of Highway Bridges: An LRFD Approach*, 3rd ed. Hoboken, NJ, USA: John Wiley & Sons Ltd, 2013.

[17] N. K. Shawki Ali, S. Y. Mahfouz, and N. H. Amer, "Flexural Response of Concrete Beams Reinforced with Steel and Fiber Reinforced Polymers," *Buildings*, vol. 13, no. 2, Jan. 2023, Art. no. 374, https://doi.org/10.3390/buildings13020374.

[18] D. V. Duc, "Local investigation and analysyses on concrete bridge deck's suspension cable anchorage area of Phat Tich-Dai Dong Thanh with application of nonlinear FE model," *Transport and Communications Science Journal*, vol. 74, no. 2, pp. 160–174, Feb. 2023, https://doi.org/10.47869/tcsj.74.2.6.

[19] H. V. Hai, "Experimental and numercal study on tensile behavior of ultra high-performance concrete," *Transport and Communications Science Journal*, vol. 74, no. 6, pp. 709–717, Aug. 2023, https://doi.org/10.47869/tcsj.74.6.2.